# First-Principles Mobility Calculations and Atomic-Scale Interface Roughness in Nanoscale Structures

M. H. Evans,[1,2] X.-G. Zhang,[3] J. D. Joannopoulos,[1] and S. T. Pantelides[2,4]

[1]*Department of Physics, Massachusetts Institute of Technology, Cambridge, Massachusetts, 02139, USA*
[2]*Department of Physics and Astronomy, Vanderbilt University, Nashville, Tennessee, 37235, USA*
[3]*Computer Science and Mathematics Division, Oak Ridge National Laboratory, Oak Ridge, Tennessee, 37831, USA*
[4]*Condensed Matter Sciences Division, Oak Ridge National Laboratory, Oak Ridge, Tennessee, 37831, USA*

(Received 20 April 2005; published 2 September 2005)

Calculations of mobilities have so far been carried out using approximate methods that suppress atomic-scale detail. Such approaches break down in nanoscale structures. Here we report the development of a method to calculate mobilities using atomic-scale models of the structures and density functional theory at various levels of sophistication and accuracy. The method is used to calculate the effect of atomic-scale roughness on electron mobilities in ultrathin double-gate silicon-on-insulator structures. The results elucidate the origin of the significant reduction in mobility observed in ultrathin structures at low electron densities.

DOI: 10.1103/PhysRevLett.95.106802 PACS numbers: 73.50.Bk, 73.40.Qv, 73.50.Dn, 73.50.Gr

A key property of semiconductors is the carrier mobility, the conductance normalized by the carrier density. In a metal-oxide-semiconductor (MOS) structure, one is interested in the mobility of carriers in the semiconductor channel adjacent to the oxide as a function of gate bias. Mobilities encapsulate all the scattering processes that influence the carriers and provide a measure of how ''fast'' an average carrier can traverse the structure. All calculations of mobilities in MOS devices have so far relied on approximations that suppress atomic-scale detail. Electrons and holes in the semiconductor are treated as classical particles whose kinetic energy is given either by the effective-mass approximation [1] or by the full energy bands [2–4]. The semiconductor-oxide interface is represented by an infinite potential wall so that carriers do not penetrate into the oxide at all [5]. Interface roughness models [6–8] assume small, continuous variations in the interface position.

As MOS structures have entered the nanoscale regime, the approximations described above are no longer adequate. Electron mobilities in strained-Si MOS structures are much larger than expected on the basis of the so-called universal mobility curve (UMC) [9–12], but state-of-the-art calculations cannot account for the deviations [13]. Mobilities in ultrathin silicon-on-insulator (UTSOI) structures [14–17] are much smaller than expected on the basis of the UMC at low carrier densities. The effect has been modeled as enhanced scattering from surface roughness using phenomenological models that include wave function penetration into the gate dielectric as a way to treat interface roughness at a more fundamental level [18,19]. The ultimate need for mobility calculations that include full atomic-scale detail and accurate wave functions is best illustrated by the following. In UTSOI structures, in which the silicon channel can be as thin as 1 nm, a single Si-O-Si bond on the silicon side of an otherwise abrupt interface changes the channel thickness by 25%. The effect on mobilities of such atomic-scale interface roughness has not been addressed so far.

In this Letter, we report the development of a method to calculate mobilities using atomic-scale models of ultrathin MOS structures and density functional theory (DFT) at various levels of sophistication and accuracy. Calculating the mobility entails solving a scattering problem; the first step is to find the relevant wave functions $\{\Psi_{nk}\}$, energy bands $\{\epsilon_{nk}\}$, and self-consistent potential $V_{\mathrm{ref}}$ for a reference ''unperturbed'' system. Next, a defect or impurity is introduced, and the system's self-consistent potential $V_{\mathrm{def}}$ in the presence of this scattering center is calculated. The self-consistent scattering potential $\Delta V$ can then be constructed: $\Delta V = V_{\mathrm{def}} - V_{\mathrm{ref}}$. Using $\Delta V$ and the unperturbed states, the scattering problem can be solved and the mobility calculated at various levels of sophistication. We apply the method to the problem of atomic-scale interface roughness in double-gate UTSOI MOSFETs, as distinct from the long-wavelength roughness that has so far been included in phenomenological mobility models. We find that atomic-scale roughness limits carrier mobilities at large carrier densities, but the effect is greatly reduced at low densities. These results corroborate earlier proposals [15,20] that long-wavelength roughness may be responsible for the observed reduction of mobilities in UTSOI MOSFETs at low electron densities. Improved processing and fabrication of UTSOI MOSFETs, as well as a reduction in channel lengths, can reduce the severity of long-wavelength thickness fluctuations and lead to as much as a 100% increase in mobility.

The present calculations were based on DFT [21] in the local density approximation (LDA) [22], used a plane-wave basis [23], and represented the ionic cores with ultrasoft pseudopotentials [24], as implemented in the VASP code [25]. For UTSOI structures, the unperturbed system is a supercell with an ideal, abrupt Si-$SiO_2$ interface, as shown in Fig. 1. The relevant bands and wave functions are

 

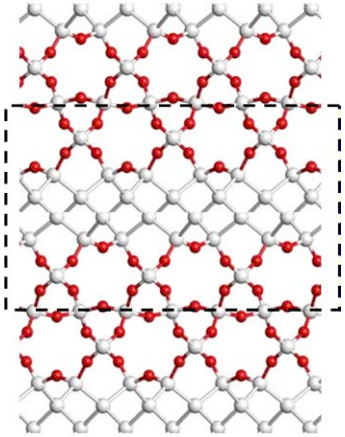

FIG. 1 (color online). Supercell containing a 5 Å-thick UTSOI silicon channel with ideal, abrupt Si-$SiO_2$ interfaces.

those at the bottom of the conduction band for electron carriers, and those at the top of the valence band for holes. Although the LDA underestimates the band gap of Si, the conduction band dispersion is reproduced accurately, making the group velocities reliable [see, for example, Fig. 1 of Ref. [26] ].

In a symmetric double-gate MOSFET, both the front and back gate are biased symmetrically such that the potential on the front and back interfaces of the silicon channel are equal, but raised or lowered with respect to the source potential [27]. In the present calculation, excess electrons (holes) are introduced into the conduction (valence) band to provide the carrier density $n_c$, and the resulting electron density and electrostatic potential are calculated self-consistently. In order to subtract out the contribution of the compensating uniform background charge and recover the proper electrostatics of the channel, we introduce an external potential that satisfies the boundary conditions appropriate to symmetrically biased gates. For a uniform background charge density $n_{bg}(= n_c)$, the external potential is: $\phi_{ext} = (en_{bg}/2\epsilon_0)z^2$, where the $z$ axis is perpendicular to the Si-$SiO_2$ interface. With this external potential, the exact conduction and valence band wave functions for the symmetric double-gate UTSOI structure can be calculated within the periodic supercell.

Once we have the reference unperturbed states and a scattering potential, we can calculate the mobility at various levels of sophistication. The most straightforward way is to solve the Boltzmann equation to linear order in the applied source-drain electric field [28,29]. The mobility $\mu_{\alpha\beta}$ for an applied voltage in the $\alpha$ direction resulting in a current in the $\beta$ direction is given by:

$$\mu_{\alpha\beta} = -e\sum_n \int \frac{d^2k}{(2\pi)^2}\tau_n(\vec{k})(\vec{v}_n(\vec{k}))_\alpha(\vec{v}_n(\vec{k}))_\beta \frac{\partial f_0(\epsilon_n(\vec{k}))}{\partial \epsilon}, \tag{1}$$

where $\vec{v}_n(\vec{k}) = \vec{\nabla}_k \epsilon_n(\vec{k})/\hbar$ is the group velocity and $\tau_n(\vec{k})$ the lifetime of state $(n\vec{k})$, and $f_0(\epsilon)$ is the equilibrium Fermi distribution. The group velocities and lifetimes contain the physics of the MOS structure, and are calculated from first principles.

The finite lifetime of a state is a result of scattering off of defects, impurities, and phonons in the MOS structure. This Letter will focus on defect and impurity scattering. A novel dynamical method for calculating mobilities due to phonon scattering will be reported in a later paper. If correlated scattering from multiple defects or impurities does not occur, the scattering rates for multiple defects or impurities simply add [29]. If we wish to include correlated scattering events, multiple defects or impurities can be included in the supercell, and the scattering potential $\Delta V$ will reflect the influence of the group of scatterers. Adding the scattering rates for a density $n_d$ of defects or impurities gives the inverse lifetime of state $(n\vec{k})$ as:

$$\frac{1}{\tau_n(\vec{k})} = n_d \sum_m \int \frac{d^2k'}{(2\pi)^2} R_{mn}(\vec{k}', \vec{k})(1 - \cos\theta), \tag{2}$$

where $\theta$ is the angle between $\vec{v}_m(\vec{k}')$ and $\vec{v}_n(\vec{k})$. Fermi's Golden Rule gives the rate of scattering from the state $(m\vec{k}')$ to state $(n\vec{k})$ under the influence of a single defect or impurity:

$$R_{mn}(\vec{k}', \vec{k}) = \frac{2\pi}{\hbar}|T_{mn}(\vec{k}', \vec{k})|^2 \delta(\epsilon_n(\vec{k}) - \epsilon_m(\vec{k}')). \tag{3}$$

The final quantity to evaluate is the scattering matrix $T_{mn}(\vec{k}', \vec{k})$, which gives the probability amplitude for scattering from the state $(m\vec{k}')$ to state $(n\vec{k}')$. Within the Born approximation:

$$T_{mn}(\vec{k}', \vec{k}) = \langle n\vec{k}|\Delta V|m\vec{k}'\rangle. \tag{4}$$

This expression for the scattering matrix contains the accurate wave functions and atomic-scale details of the MOS structure, and enables direct comparison with existing mobility models. To go beyond the Born approximation, we define a Hamiltonian in second-quantized notation that contains all of the physics described above:

$$H = \sum_{nk} \epsilon_n(\vec{k}) c^\dagger_{nk} c_{nk} + \sum_{mk}\sum_{nk'} S(\vec{k}' - \vec{k}) \times \langle n\vec{k}'|\Delta V|m\vec{k}\rangle c^\dagger_{nk'} c_{mk}. \tag{5}$$

The structure factor $S(\vec{k}) = \sum_{R_d} \exp(-i\vec{k}\cdot\vec{R}_d)$ contains all information about the random defect or impurity positions $\{\vec{R}_d\}$. Given this Hamiltonian, we can solve for the finite-temperature (Matsubara) Green's function $G_{mn}(\vec{k}, \vec{k}', i\omega)$ [29], which encapsulates all transport and scattering properties of the carriers. The Kubo formula can then be used to calculate the mobility tensor $\mu_{\alpha\beta}$. Applications of standard Green's function techniques to this Hamiltonian will be discussed in a later paper.

Previous work [30] has identified the elemental defects that contribute to interface roughness (Fig. 2): a Si-Si bond

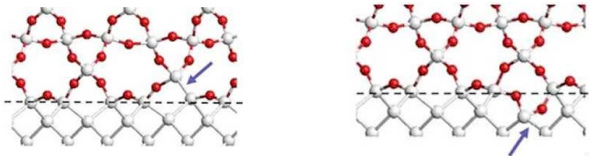

FIG. 2 (color online). Schematics of an Si-$SiO_2$ interface showing elementary interface roughness defects: suboxide bond (left) and oxygen protrusion (right).

on the oxide side of the interface, called a *suboxide bond*, and an Si-O-Si bond on the silicon side of the interface, called an *oxygen protrusion*. A combination of these two defects leads to a fluctuating interface. We have calculated relaxed suboxide bond and oxygen protrusion structures for channels with thicknesses ranging from 10–25 Å. Using these structures, the scattering matrix was calculated via Eq. (4) and the mobility was calculated from Eq. (1). Figure 3 shows the self-consistent scattering potentials for the oxygen protrusion and suboxide bond in a 10 Å channel, together with the conduction electron density of $5.6 \times 10^{12}$ $e^-/cm^2$. The oxygen protrusion consists of an additional oxygen ion, and so provides an attractive potential on the silicon side of the interface. The suboxide bond, a missing oxygen ion, leads to a repulsive potential on the oxide side.

Figure 4 shows the calculated mobilities due to suboxide bonds and oxygen protrusions for 10 Å-, 15 Å-, and 20 Å-thick channels at 300 K. The density of both suboxide bonds and oxygen protrusions is taken to be $2.2 \times 10^{11}$ defects/$cm^2$, the same order of magnitude as observed interface trap densities [15]. The defect density will in general depend on film growth and device processing conditions, but as shown by Eq. (2), the defect density only provides an overall scaling factor for the mobilities.

A surprising feature of Fig. 4 is the fact that oxygen protrusion-limited mobilities are consistently larger than suboxide bond-limited mobilities, despite the fact that the oxygen protrusion lies within the silicon channel. The explanation for this result lies in the $sp^3$-antibonding character of the states at the bottom of the conduction band in

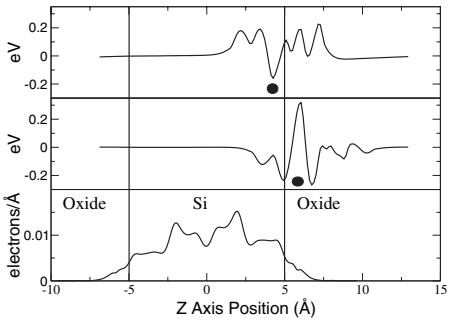


FIG. 3. Plot showing plane-averaged scattering potentials for oxygen protrusions (top) and suboxide bonds (middle), along with carrier density (bottom). The $z$ axis is perpendicular to the Si-$SiO_2$ interface. Black circles mark the defect centers.

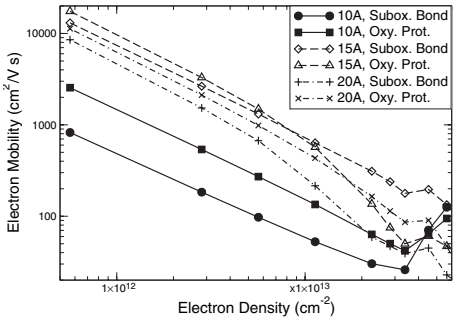


FIG. 4. Calculated electron mobilities due to scattering from suboxide bonds and oxygen protrusions for channel thicknesses of 10, 15, and 20 Å at 300 K.

silicon. The extra oxygen atom that constitutes the protrusion lies near the middle of the Si-Si bond, where an $sp^3$-antibonding wave function has a node, reducing the overlap with the scattering potential. Figure 5 shows that this intuition is valid for a UTSOI channel.

The electron mobility measured in UTSOI MOSFETs remains constant or even decreases with decreasing electron density in the $\lesssim 10^{13}$ $e^-/cm^2$ range, falling well below the UMC [14–17]. Theoretical work [8,18,31], based on interface roughness models that consider the interface position to fluctuate gradually over many nanometers, has reproduced qualitatively this UMC deviation. In the following discussion, we will refer to scattering caused by these interface fluctuations as "long-wavelength roughness scattering." The present model, based on atomic-scale defects, reflects short-wavelength roughness. As pointed out by Uchida *et al.* [14] and Ernst *et al.* [20], it is difficult to fabricate UTSOI MOSFETs with uniform channel thickness. Suboxide bonds and oxygen protrusions, on the other hand, are elemental interface roughness defects that will likely always be present due to strain at the Si-$SiO_2$ interface [30,32]. As shown in Fig. 4, the mobility for suboxide bonds and oxygen protrusions at all channel thicknesses is proportional to $1/n_e$ for low conduction electron densities ($n_e \lesssim 10^{13}$ $e^-/cm^2$).

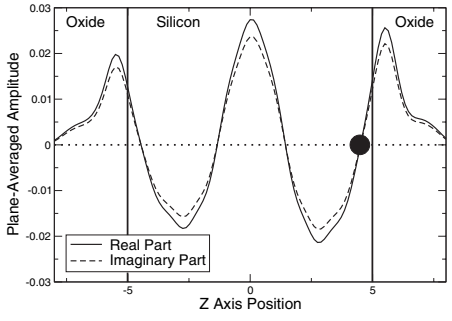


FIG. 5. Plane-averaged wave function at the bottom of the conduction band in a 10 Å-thick UTSOI channel. The conduction electron density in the channel is $5.6 \times 10^{11}$ $e^-/cm^2$. The $z$ axis is perpendicular to the Si-$SiO_2$ interface. A black circle marks the center of the oxygen protrusion.

Simulations of a 25 Å-thick UTSOI channel based on Esseni's interface roughness scattering model [18] show that at room temperature and electron densities below $10^{13}$ $e^-/cm^2$, the phonon and long-wavelength roughness scattering contributions to the mobility are roughly equal. As a result, the total mobility, given by Mathiessen's rule, is: $1/\mu_{tot} = 1/\mu_{phonon} + 1/\mu_{LWR} \approx 2/\mu_{phonon}$, where $\mu_{LWR}$ is the mobility due to long-wavelength roughness scattering. If improved device fabrication processes can reduce or eliminate long-wavelength interface thickness fluctuations, only short-wavelength roughness due to oxygen protrusions and suboxide bonds will remain. Thus: $1/\mu_{tot} = 1/\mu_{phonon} + 1/\mu_{SWR} \approx 1/\mu_{phonon}$, since $1/\mu_{SWR} \approx 0$ at low electron densities. Because of the $1/n_e$ dependence of the short-wavelength roughness mobility, reducing UTSOI channel thickness fluctuations could result in up to a 100% gain in mobility at low carrier densities.

In addition to the room-temperature data, there also exist measurements of resistivity in bulk Si MOSFETs, where anomalous behavior has been observed for very low carrier densities ($<2 \times 10^{11}$ $e^-/cm^2$) in the range 0–3 K [33]. This behavior has been explained in a recent Letter by Punnoose and Finkel'stein [34] in terms of electron-electron interactions. The explanation is applicable to the case of a wide channel, which suppresses interface roughness (IR) scattering. There are no data for UTSOI devices, where the Si-$SiO_2$ interfaces constrain the channel width and prevent the automatic suppression of IR scattering. Indeed, we note that the $1/n_e$ dependence of the mobility at low densities (Fig. 4) leads to a density-independent contribution to the resistivity. Low-temperature and low-density data in UTSOI devices would be useful to probe the extent to which the electron-electron interaction treated in Ref. [34] can give rise to observable effects even though IR scattering is not suppressed.

In conclusion, we have reported a novel first-principles method for the calculation of defect and impurity-limited mobilities in MOS structures. Accurate wave functions, energy bands, and interface structures allow a direct connection to be made between atomic-scale processes and the measured electrical response of devices. A new atomic-scale model of interface roughness scattering was developed based on this method, and it was demonstrated that the significant reduction in low-electron-density mobilities observed in UTSOI MOSFETs are due to long-wavelength channel thickness fluctuations, and not to scattering from elemental interface roughness defects. Improved device fabrication processes that reduce or eliminate these long-wavelength fluctuations could result in a mobility increase of up to 100%.

The authors would like to thank Dr. Kalman Varga of Oak Ridge National Laboratory and Professor Ron Schrimpf of Vanderbilt University for valuable discussions. This work was supported in part by the Department of Energy Grant No. DE-FG02-03ER46096 and by the William A. and Nancy F. McMinn Endowment at Vanderbilt University. Work at Oak Ridge National Laboratory (ORNL) was funded by LDRD. ORNL is operated by UT-Battelle, LLC, for the U.S. Department of Energy under Contract No. DE-AC05-00OR22725. Computations were performed on the National Science Foundation Terascale Computing System at the Pittsburgh Supercomputer Center.

[1] T. Ando, A. B. Fowler, and F. Stern, Rev. Mod. Phys. **54**, 437 (1982), see Section III.
[2] M. V. Fischetti and S. E. Laux, Phys. Rev. B **38**, 9721 (1988).
[3] M. V. Fischetti and S. E. Laux, Phys. Rev. B **48**, 2244 (1993).
[4] P. Yoder and K. Hess, Semicond. Sci. Technol. **9**, 852 (1994).
[5] F. Stern and W. E. Howard, Phys. Rev. **163**, 816 (1967).
[6] T. Ando, J. Phys. Soc. Jpn. **43**, 1616 (1977).
[7] S. Yamakawa *et al.*, J. Appl. Phys. **79**, 911 (1996).
[8] F. Gamiz *et al.*, J. Appl. Phys. **86**, 6854 (1999).
[9] F. Gamiz *et al.*, IEEE Trans. Electron Devices **42**, 258 (1995).
[10] K. Chen *et al.*, IEEE Electron Device Lett. **17**, 202 (1996).
[11] S.-I. Takagi *et al.*, IEEE Trans. Electron Devices **41**, 2357 (1994).
[12] S. Villa *et al.*, IEEE Trans. Electron Devices **45**, 110 (1998).
[13] M. Fischetti, F. Gamiz, and W. Hansch, J. Appl. Phys. **92**, 7320 (2002).
[14] K. Uchida *et al.*, *IEDM Technical Digest*, 47 (2002).
[15] K. Uchida, J. Koga, and S. Takagi, *IEDM Technical Digest*, 805 (2003).
[16] D. Esseni *et al.*, IEEE Trans. Electron Devices **50**, 802 (2003).
[17] M. Prunnila, J. Ahopelto, and F. Gamiz, Appl. Phys. Lett. **84**, 2298 (2004).
[18] D. Esseni, IEEE Trans. Electron Devices **51**, 394 (2004).
[19] I. Polishchuk and C. Hu, *VLSI Technology Digest of Technical Papers*, 51 (2001).
[20] T. Ernst *et al.*, IEEE Trans. Electron Devices **50**, 830 (2003).
[21] P. Hohenberg and W. Kohn, Phys. Rev. **136**, B864 (1964).
[22] W. Kohn and L. Sham, Phys. Rev. **140**, A1133 (1965).
[23] M. C. Payne *et al.*, Rev. Mod. Phys. **64**, 1045 (1992).
[24] D. Vanderbilt, Phys. Rev. B **41**, R7892 (1990).
[25] G. Kresse and J. Furthmüller, Phys. Rev. B **54**, 11169 (1996).
[26] J. Gryko and O. F. Sankey, Phys. Rev. B **51**, 7295 (1995).
[27] Y. Taur, IEEE Trans. Electron Devices **48**, 2861 (2001).
[28] J. M. Ziman, *Electrons and Phonons* (Oxford University, New York, 1960).
[29] G. Mahan, *Many-Particle Physics* (Plenum, New York, 1990), 2nd ed..
[30] R. Buczko, S. J. Pennycook, and S. T. Pantelides, Phys. Rev. Lett. **84**, 943 (2000).
[31] D. Esseni *et al.*, *IEDM Technical Digest*, 719 (2002).
[32] A. Bongiorno *et al.*, Phys. Rev. Lett. **90**, 186101 (2003).
[33] V. M. Pudalov *et al.*, Physica E (Amsterdam) **3**, 79 (1998).
[34] A. Punnoose and A. M. Finkel'stein, Phys. Rev. Lett. **88**, 016802 (2002).